# Structuring of Photosensitive Polymer Brushes

*Alexey Kopyshev,[1] Katerina Kanevche,[2] Nino Lomadze,[1] Emanuel Pfitzner [2] Sarah Loebner [1]*

*Rohan R. Patil [3] Jan Genzer,[3] Joachim Heberle,[2] Svetlana Santer[1]*

[1] Experimental Physics, Institute of Physics and Astronomy, University of Potsdam, Karl-Liebknecht Str. 24, 14476 Potsdam, Germany

[2] Experimental Molecular Biophysics, Department of Physics, Freie Universität Berlin, Arnimallee 14, 14195 Berlin, Germany

[3] Department of Chemical & Biomolecular Engineering, North Carolina State University, Raleigh, NC 27695-7905, USA

AUTHOR EMAIL ADDRESS: santer@uni-potsdam.de

**RECEIVED DATE**

TITLE RUNNING HEAD: Photosensitive brushes, photosensitive azobenzene containing surfactants, strong polyelectrolyte brush

ABSTRACT

We investigate light-induced irreversible structuring of surface topographies in poly(3-sulfopropyl methacrylate / potassium salt) (PSPMK) brushes on flat solid substrates prepared by surface-initiated atom transfer radical polymerization that have been loaded with azobenzene-based surfactants comprising positively charged head groups and hydrophobic tails. The surfactants exhibit photo-responsive properties through photo-isomerization from the *trans*- to *cis*- states leading to significant changes in physico-chemical properties of grafted polymer chains as a whole such as polarity, size and shape. Exposing these photosensitive brushes to irradiation with UV interference beams causes the polymer brush to form surface relief grating (SRG) patterns. The cationic surfactant functionalizes penetrate only ~25% of the upper portion of the PSPMK brush, resulting in the formation of two sections within the brush: a photo-responsive upper layer and non-functional buried layer, which is not affected by the UV irradiation. Using nanoFTIR spectroscopy, we characterize locally the chemical composition of the polymer brush, and confirm partial penetration of the surfactant within the film. Strong opto-mechanical stresses take place only within the upper layer of the brush that is impregnated with the surfactants and causes surface topography alternation due to a local rupture of grafted polymer chains. The cleaved polymer chains are then removed from the surface using a good solvent, leaving behind topographical grating on top of the non-functional brush layer. Photo-structured polymer brush can be used for reversible switching of brush topography by varying external humidity. The azobenzene surfactant enables photo-responsive behavior without introducing irreversible changes to chemical composition of the parent polymer brush.

## Introduction

A polymer brush features polymer chains attached covalently with one end to a solid surface at high grafting density (*i.e.*, a number of polymer grafts per unit area). Such a system allows for tailoring surface properties for specific applications in biomedicine, nanotechnology, bioelectronics, optics, and other fields.[1,2,3,4,5,6,7,8,9] The density of the anchoring points at which chains can be "grafted" ranges typically from 0.01 to 0.5 chains/nm$^2$.[10,11,12,13,14] The chemical structure, grafting density, and the molecular weight of the polymer chains governs the brush properties. Brushes consisting of polymer chains with ionizable groups are referred to as polyelectrolyte (PE) brushes.[15,16,17,18,19] They exhibit a strong dependence on the density of ionized/ionizable groups and the concentration of external salt in solution to which they are exposed. The PE brushes have received recently attention due to generating responsive coatings.[20] One practical advantage of PE brushes is the possibility to modify them *posteriori* by attaching modifiers that alter the original characteristic of the grafted polymer. In this way, the brush can be made to interact with proteins or nano-particles or even be loaded with other small molecules through electrostatic or other physical/chemical interactions.[21,22,23,24,25,26,27,28,29,30,31] For instance, a negatively charged polyelectrolyte brush (*i.e.*, poly(methacrylic acid)) exposed to a solution containing cationic photoresponsive surfactant may uptake a significant amount of surfactant molecules.[32] The surfactant may include a positively charged head group and a hydrophobic tail group containing an azobenzene group, which can undergo reversible photo-isomerization from a *trans*- to a *cis*-conformation rendering surfactant either hydrophobic or hydrophilic, respectively.[33,34,35] When the polymer brush modified by photosensitive moieties is exposed to an irradiation using interference pattern (IP), *i.e.*, light with periodically varying intensity or polarization, the topography of the brush alters brush topography while forming the

so-called surface relief gratings (SRG) featuring a sinusoidally-shaped profile that propagates up to several hundreds of nanometers in depth. This phenomenon has been observed first in physisorbed polymer films[36,37] and later in polymer brushes.[38,39] The SRG mechanism in glassy polymer materials results in the generation of strong, internal opto-mechanical stresses which can be as high as 1 GPa. [40,41,42,43] The macroscopic viscoplastic deformations of the solid material (Young modulus of the polymer film is several GPa) is governed by local ordering of the azobenzene groups that re-orient perpendicularly to the electrical field vector during the IP irradiation. As a consequence, the polymer backbones follow local changes in the orientation of azobenzenes, to which they are attached.[44] In polymer brushes, the high grafting density leads to significant stretching of chains; the extent to which backbones can reorient or migrate is limited. Thus, the SRG formation can be accompanied by local rupturing or scission of polymer chains in areas from which the polymer material is receding, *i.e.*, in the SRG minima. By exposing the structured brush to a good solvent the ruptured chains can be liberated from the surface by exposing the irradiated substrate to a good solvent, thus leaving behind characteristic topographical patterns as a footprint of the irradiation event. Due to the high grafting density of polymer brushes, the surfactant may not penetrate completely throughout the entire brush thickness (*i.e.*, the bottom portion of the brush remains unfunctionalized). The depth, to which the surfactant can penetrate into the brush, also depends on the surfactant size. Thus, surfactants with longer spacer groups connecting the head-group and the azobenzene unit will impregnate the brush only to a limited extent.[45] During the SRG process the rupturing of polymer chains occurs predominantly in the surface regions that possess high concentration of the surfactant. In the past we also studied the SRG process using diblock-copolymer brushes consisting of poly(methylmethacrylate-b-methacrylic acid) (PMMA-b-PMAA), in which the top block was

functionalized with the azobenzene surfactant. We reported that rupturing occurred at the link connecting the bottom PMMA (non-functionalized) and the top PMAA (photosensitive) blocks. [32] The results described above utilized PMAA polyelectrolyte brushes of grafting densities between 0.01 and 0.4 chains/nm$^2$, showing that this parameter does not influence significantly the functionalization of the brush with the oppositely charged surfactant.

The PMAA brush is a so-called weak PE brush, in which the degree of dissociation depends on local environmental conditions, *i.e*, the pH, and ionic strength, both of which can tune the charge densities along the polymer chains.[46,47,48,49] In contrast, the so-called strong PE brushes have a fixed number and positions of the charges along the backbone, *i.e.*, there is no significant change in the brush conformation in response to pH (in salt-free solution).[50,51,46] In salt free (at neutral pH) solution the difference between the weak and strong PE brush can be understood as follows. In weakly charged PE brushes, the counter ions may leave the interior of the brush and the osmotic pressure of the counter ions becomes negligible in comparison to uncompensated electrostatic repulsion between charged monomers along the polymer chains. In strong PE brushes, nearly all counter ions are localized in the brush interior, which results in a high osmotic pressure within the polymer film. In response to releasing this pressure, the confinement of the counter ions in strong PE brushes leads to significant swelling of the charged polymers due to water uptake under salt free conditions. The difference in counter ion distribution gives rise to different interactions with small charged objects, such as proteins, nano-particles, and surfactant molecules.[52]

Here we report on a complex formation involving strong polyelectrolyte brushes comprising poly(3-sulfopropyl methacrylate / potassium salt) (PSPMK) and photosensitive surfactants. The cationic surfactant penetrates only ~25% of the upper region of the brush (*vide*

*infra*), resulting in two distinct layers: a photo-responsive upper layer and a surfactant-free region, which remains unaffected by irradiation. We have found that during the formation of SRGs in a photosensitive PSPMK brush, opto-mechanically induced scission of polymer chains takes place only within the portion of the brush that possesses high surfactant concentration. We have applied nanoFTIR spectroscopy [59, 61] which is an optical near-field technique not limited by diffraction. [62-66, 70] to characterize the chemical composition of the polymer brush at a spatial resolution of 30 nm, and confirm the partial penetration of the surfactant. Finally, we show that after undergoing photo-structuring the polymer brush can be further reversibly manipulated by modifying the brush topography through variation in humidity.

## Experimental Part

### Materials

Poly(3-sulfopropyl methacrylate / potassium salt) *(PSPMK) brushes* were synthesized using a surface-initiated atom transfer radical polymerization (ATRP).[40] In the first step, a silicon wafer was modified with 11-(2-bromo-2-methyl)propionyloxy)undecyl-trichlorosilane (BMPUS) ATRP initiator using a previously reported protocol,

Azobenzene containing trimethylammonium bromide surfactant (Azo-Nitro-TMAB) (**Figure 1**) was synthesized by the reaction of 4-(4-Nitrophenylazo)phenol with 1,6-dibromohexane and subsequent quaternization with trimethylamine, as described elsewhere.[33] The surfactant was dissolved in water (MilliQ) and kept in dark for several days to ensure complete relaxation to the *trans* configuration. All experiments were carried out in a room with yellow light to avoid any premature isomerization of the surfactant.

*Binding of photosensitive surfactants.* The PSPMK brushes were placed in surfactant solutions of a given concentration for 0.5 hour at room temperature followed by rinsing with water and drying under nitrogen flow.

**Methods**: Atomic Force Microscopy (AFM) (Nanoscope V, Veeco), in tapping mode using commercial tips (NanoSensors) with a resonance frequency of 300 kHz and a spring constant of ~50 N/m, was utilized to characterize the thickness and morphology of the polymer brushes. The measurements were carried out in air, at room temperature, and constant humidity of 55%. For thickness measurements, the brush was scratched with a glass pipette to completely remove polymer material from the substrate and the height between the top of the brush and the substrate was analyzed from the AFM cross-section data.

To achieve photoinduced deformation in polymer brushes, we employed a two beam interferometer irradiation; the light source consists of a continuous (pumped with wave-diode) solid state laser (CW-DPSSL, 75mW output power) operating in a single longitudinal mode with a wavelength of 491 nm, oscillating in vertical linear polarization state (↕) (Cobalt Calypso$^{TM}$). The laser beam is spatially expanded and then collimated with a pair of focusing and collimating lenses and a pinhole system. A 50:50 (L:R) beam splitter is placed behind the pinhole to split the single into two beams with roughly equal intensities. The beams then pass through a set of wave plates and polarizers and interfere near the polymer surface. Irradiation impinges onto the brush.

Near-Field Fourier-Transformed Infrared (nanoFTIR) spectroscopy. A home-built near-field spectrometer with an asymmetric Michelson interferometer configuration [53, 54, 55] was employed to record infrared spectra at nm-spatial resolution. The system is equipped with a femtosecond laser source (FemtoFiber dichro midIR, NeaSpec GmbH, Germany) focused on an

Atomic Force Microscope (AFM) (NanoWizard II, JPK instruments AG, Germany) tip (Arrow NC Pt, NanoWorld, Germany) and a mercury cadmium telluride (MCT) detector (KLD-0.1-J1/DC/11, Kolmar Technologies Inc., USA). The AFM is operated in tapping mode at the tip's resonance frequency of 285 kHz. The detected near-field signal is demodulated at higher harmonics of the tip's tapping frequency via lock-in amplifier (HF2LI, Zurich Instruments, Switzerland) to suppress background scattering and to extract the near-field contribution.[54] Interferometric detection delivers the scattered near-field amplitude and phase related to the sample's reflectance and absorption, respectively.[56,57]

## Results and Discussion

The scheme and chemical structure of the poly(3-sulfopropyl methacrylate / potassium salt) polyelectrolyte brush (PSPMK) loaded with azobenzene-containing cationic surfactant is depicted in **Figure 1**. The grafting density of the PSPMK brushes investigated is $\sigma$=0.24 chains/nm$^2$, and the molecular weight 570·10$^2$ kDa giving rise to the dry thickness of ~200 nm.

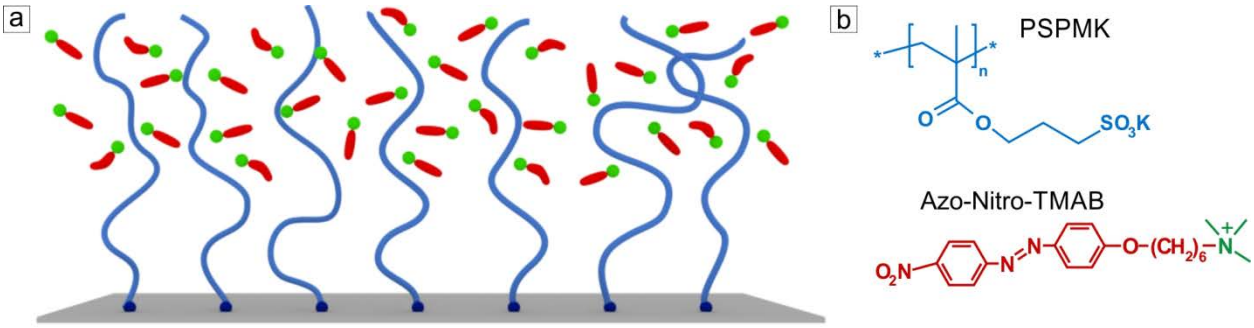


**Figure 1.** (a) Scheme of the polyelectrolyte poly(3-sulfopropyl methacrylate potassium salt) brush (PSPMK) loaded with photosenstitive surfactant. (b) Chemical structure of PSPMK brush and azobenzene containing trimethylammonium bromide surfactant (Azo-Nitro-TMAB).

After exposure to surfactant solution, the height of the brush increases almost twofold up to 400 nm. The degree of binding $\beta$=0.66 is calculated using the equation: [58]

$$\beta = \frac{\frac{h^{Azo}}{h_0} - 1}{\frac{M_0^{Azo+SPM}}{M_0^{SPMK}} - 1}, \qquad (1)$$

where $h_b$ and $h_b^{azo}$ are the brush dry thicknesses before and after complex formation, and $M_0^{SPMK}$=246 Da and $M_0^{azo+SPM}$=593 Da are the molecular weights of the repeat units before and after complexation with surfactant, respectively. This quantity can be interpreted as a normalized surfactant concentration indicating the number of surfactant molecules per SPMK monomer units in the brush. This is the maximum value possible for a strong polyelectrolyte PSPMK brush. In contrast, weak PMAA polyelectrolyte brushes were shown to absorb more cationic surfactants resulting in an increase in thickness up to 6 fold (β=1.2).[59] The difference in the amount of absorbed surfactant molecules is likely due to significant trapping of counter-ions in the interior of the strong PSPMK polyelectrolyte brush resulting in high osmotic pressure inside the brush and thus low penetration depth of the cationic surfactant.[60,61] Since only the degree of binding is known, it is not possible to conclude much about the local distribution of the surfactant within the brush film. In the following we will elucidate this point in more detail along with analyzing the characteristics of the irradiated azobenzene-containing polyelectrolyte brush.

The photoresponsive brush is irradiated with interference patterns using UV light (λ=325 nm, I=20 mW/cm$^2$) for different irradiation times ranging from 5 to 30 minutes. In this way, the energy density fed into the system varies between 6 and 36 J/cm$^2$. The polymer topography, being flat before irradiation, turns into surface relief gratings during the exposure to the interference pattern optical periodicity of D=1.9 μm (**Figure 2a**). The height of the inscribed gratings of 10±2 nm does not vary significantly with the irradiation time. This shows that the topography deformation essentially completes within the first few minutes of UV light exposure and further irradiation does not lead to any increase in the SRG height. This observation can be

explained by the fact that multiple *trans-cis* isomerizations of the azobenzene surfactant molecules within the brush matrix do not occur, but takes place as a pure process. This hinders continuous alignment of the azobenzene units perpendicular to the polarization of the incident light, necessary for further deformation of the polymer matrix. [32]

However, the reaction of the brush does not only involve a simple topography change. In our previous study we have reported that polymer chains can be cleaved at the surface during the SRG formation. This rupture process takes place only in the photosensitive part of the brush, which contains the surfactant molecules. [62] In order to comprehend the morphology of the PSPMK-Azo-Surfactant complex after irradiation the brush, we exposed the specimen to a good solvent for 10 minutes, followed by drying in nitrogen gas. **Figure 2a** shows the corresponding topography of the brush after such treatment. The height of the topography grating increases with irradiation time from 12 to 120 nm and then drops to 40 nm (**Figure 2b**). We measured the brush heights before and after the UV irradiation at a reference scratch site (see experimental section). This allows acquiring both the SRG height and the whole thickness of the brush. The experimental data reveal that the topography minima of the grating do not extend all the way down to the substrate; *i.e.*, a certain portion of the brush remains intact during the SRG process. In **Figure 2c** this latter part of the brush is displayed in grey, together with the SRG profile that is plotted in blue. The explanation of the change in the SRG height is that some of the polymer chains have been ruptured from areas where the SRG topography minima have formed during the SRG process and subsequently removed during the exposure to a good solvent. The rupture is induced by strong opto-mechanical stresses generated locally during UV irradiation with interference patterns; it does not occur under homogeneous illumination conditions as revealed

from the AFM cross-sectional analysis of the brush thickness after irradiation and subsequent treatment with a good solvent.

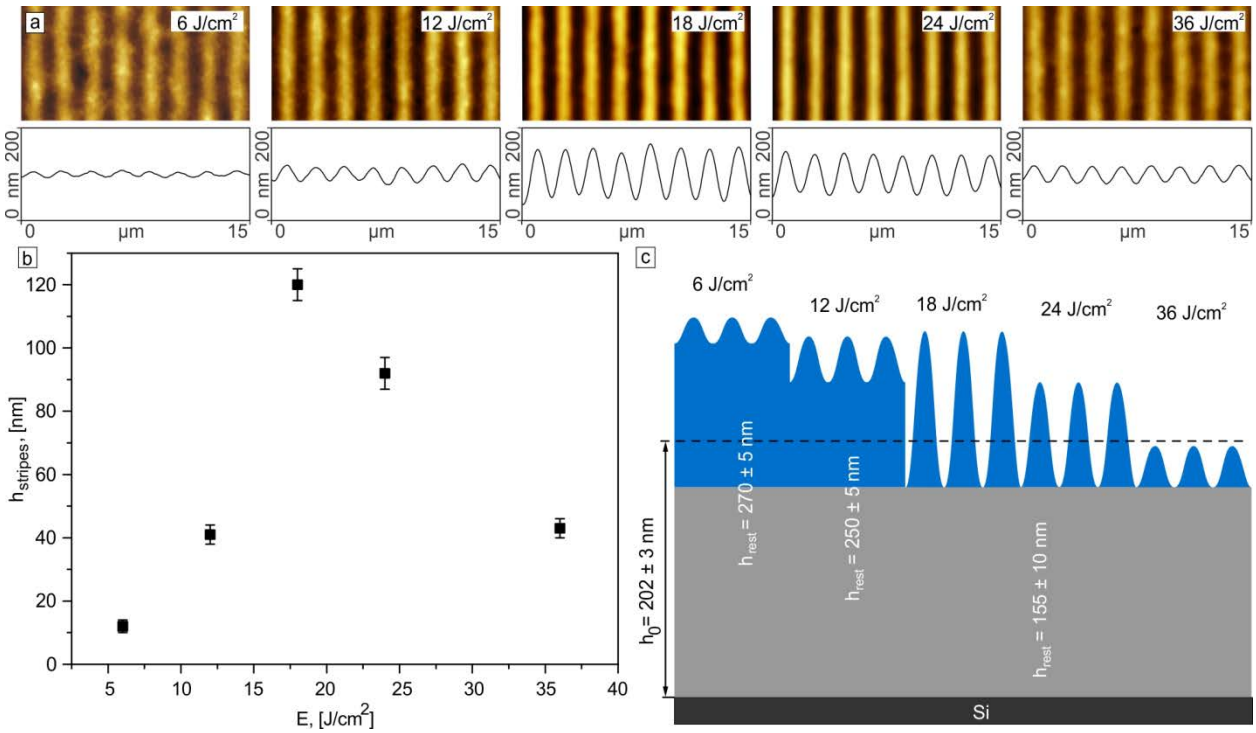


**Figure 2**. (a) AFM micrographs of the brush topography irradiated with interference patterns and subsequently treated with a good solvent (toluene). The irradiation is performed with UV (λ=325 nm) wavelength, the optical grating periodicity is D=1.9 µm with irradiation times varying from 5 to 30 minutes. (b) Dependence of the SRG height on irradiation energy/time. (c) A schematic of the brush cross section. The brush modified with azobenzene-containing surfactant is shown in blue, while the surfactant-free, i.e., unmodified, section of the brush is shown in grey.

Starting from the irradiation time of 15 minutes (energy density 18 J/cm$^2$), the cross-sectional analysis demonstrates that the thickness of the brush measured between the minimum of the stripes and the substrate (grey color in **Figure 2c**) remains constant at ~155 nm. We explain this by the fact that due to high osmotic pressure within the strong polyelectrolyte brush, the surfactant penetrates the brush only partially, *i.e.*, only the top ~50 nm of the brush layer forms a complex with the with azobenzene-containing surfactant and the bottom ~75% of the brush interior remains surfactant-free. This also explains why even under long irradiation times ~155

nm of the bottom portion of the brush remains attached to the substrate. The results presented in **Figure 2** also reveal that the height of the SRG (marked in blue) decreases at irradiation times of 20 min (energy density 24 J/cm$^2$) and 30 min (energy density 36 J/cm$^2$). This indicates that chain scission also occurs near the topography maxima, thus resulting in a decrease of the stripe height due to the removal of the ruptured chains. Using the results from **Figure 2c** one can also calculate the total number of ruptured chains using the following equation:

$$number\ of\ ruptured\ chains = \frac{S_0 - S_{irr}}{S_0} \cdot 100\%, \qquad (2)$$

where $S_0$ is the AFM cross-sectional area of the initial brush profile, and $S_{irr}$ is the AFM cross-sectional area of the brush after UV irradiation and subsequent treatment with a good solvent (**Figure 2**). The cross-sectional profile for all measurements was analyzed over a lateral distance of 15 μm, *i.e.*, ~7 SRG periods. At maximum exposure (36 J/cm$^2$ dose) more than 90% of the PSPMK chains in the photosensitive part of the brush have been ruptured, while the thickness of the remaining bottom layer (~155 nm, marked in grey in **Figure 2c**) remains constant. Thus the opto-mechanical stresses generated during the SRG formation do not "pluck" of the surfactant-free sections of the PSPMK brushes.

To prove our conjecture that the portion of the brush that remains anchored to the substrate after the SRG treatment consists of PSPMK, we performed the following experiment. The brush was irradiated a second time under identical conditions but with the intensity pattern oriented perpendicular to the first one. The irradiation dose chosen was 18 J/cm$^2$ (15 min irradiation at I=20 mW/cm$^2$, λ=325 nm) in order to obtain the maximum possible SRG height (see **Figure 2c**). After this second irradiation, only the stripes containing azobenzene surfactants (marked in blue in **Figure 3**) are modulated resulting in a square pattern, while the rest of the brush remains intact (**Figure 3**).

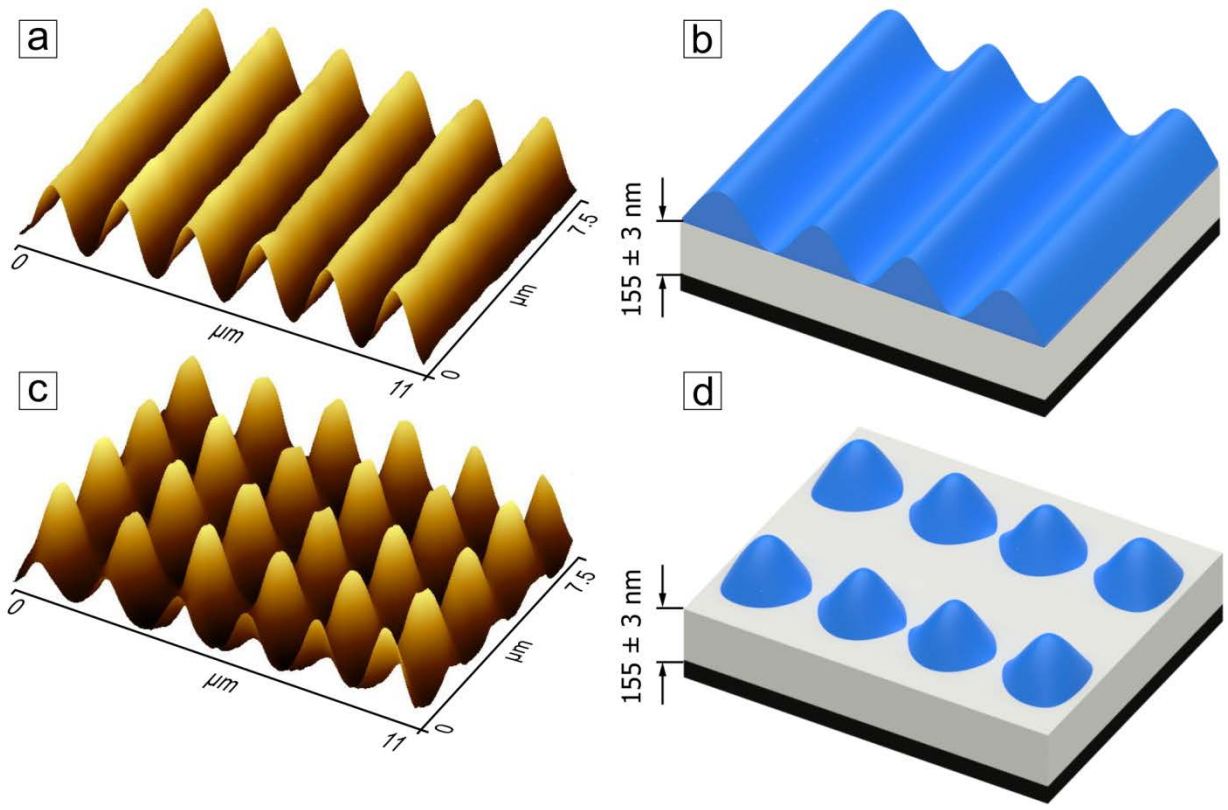


**Figure3.** (a) AFM micrographs of the irradiated brush after an initial UV irradiation with 24 J/cm$^2$ and subsequent treatment with a good solvent reveals the presence of the characteristic stripe-like SRG topography. (b) Corresponding scheme where the grey portions depict the non-modified part of the brush, while the brush sections loaded with the photosensitive surfactant are shown in blue. (c) AFM micrograph of the same brush irradiated for a second time with an interference pattern rotated by 90°, followed by exposure to a good solvent. The stripes are now reshaped forming bumps of the same optical periodicity as the interference pattern. The area between the stripes shows no response to irradiation and the thickness of the inactive part is still 155 nm (grey color in d).

For sufficiently short irradiation times, one can repeat the steps a few times. For instance, **Figure 4** demonstrates the result of three successive cross irradiations: the first exposure is to a grating with optical periodicity of 2.7 µm (**Figure 4a**) for 5 minutes (energy density 6 J/cm$^2$), followed by a second irradiation for 5 minutes with an interference pattern (IP) of 1.3 µm aligned perpendicularly to the first grating (**Figure 4b**) and in the third step the sample is rotated by 45° with respect to the second grating and irradiated with an IP of 0.8 µm (**Figure 4c**). The result of

the three irradiation steps comprises a complex pattern inscribed within the upper layer of the brush, while the rest of the (unmodified) brush has a height of 160±5 nm, similar to the result described in **Figure 2c** at a UV dose of 18 J/cm$^2$.

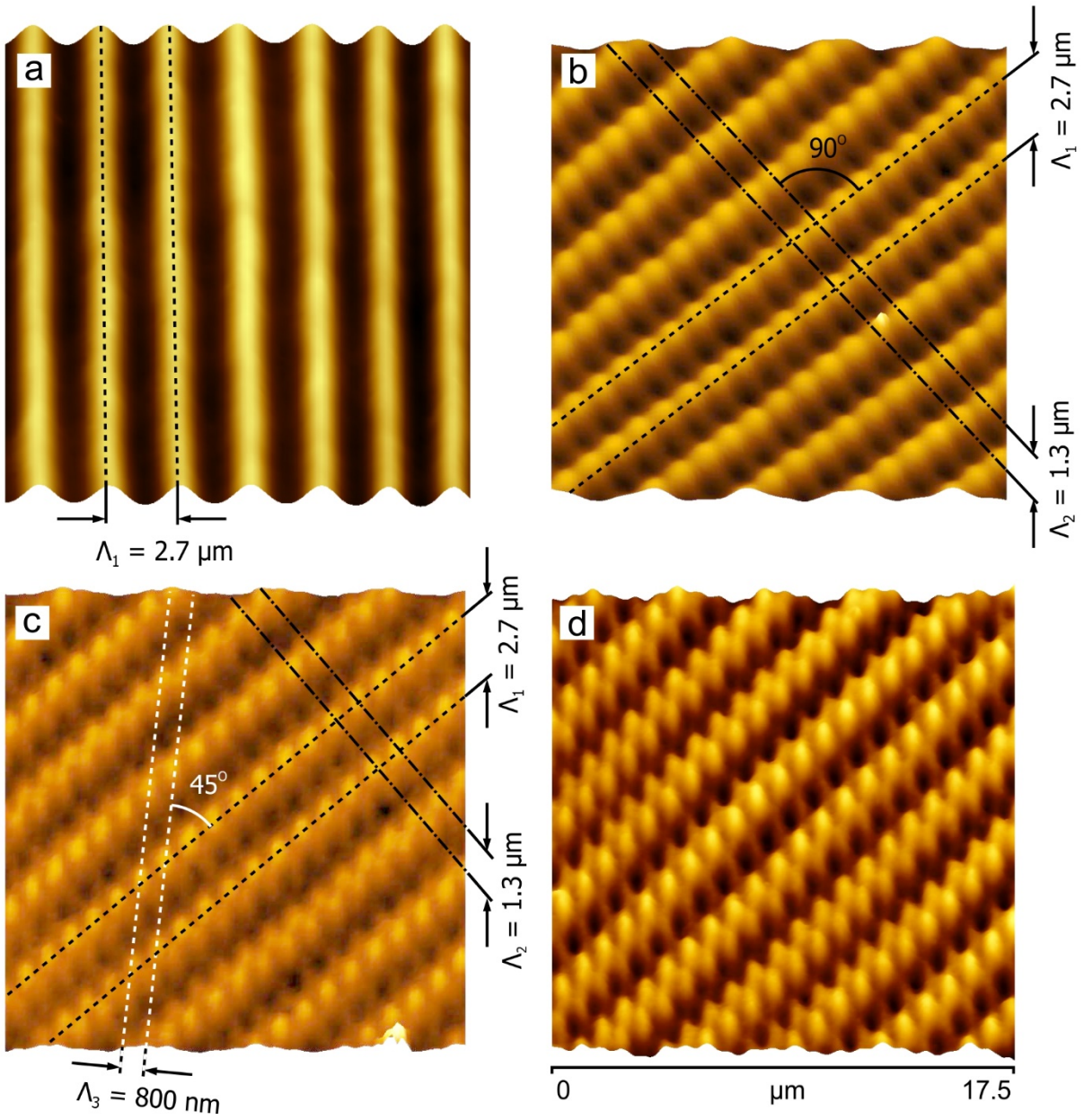


**Figure 4.** AFM micrographs of the photosensitive PSPMK brush after three irradiation steps with an interference pattern at λ = 325 nm and subsequent treatment with good solvent; the irradiation dose is 12 J/cm$^2$ at each step. (a) first irradiation, the period of the IP is 2.7 μm; (b) second irradiation perpendicular to the first one, the period of the IP is 1.3μm; (c) third irradiation oriented at 45° to the first one IP period is 0.8 μm; (d) topography of the brush from (c) replenished with azobenzene containing surfactant.

The attempt to imprint another irradiation pattern into the polymer brush with a fourth treatment cycle (irradiation+cleansing) was ineffective because most of the photosensitive molecules have been washed out form the interior of the brush during the exposure to a good solvent (DMF). The stability of what remains of the brush treated this way is remarkable, yet we are able to make it photosensitive again by replenishing the remaining brush with a new amount of a surfactant (**Figure 4d**) by exposing the brush 1 mM surfactant solution for 30 minutes followed by a rinsing and drying. After surfactant uptake, the brush height increased from ~155 to ~230 nm.

The height of the inscribed SRG pattern depends strongly not only on the irradiation dose, but also on the nature of the interference pattern. IPs are commonly categorized as intensity interference patterns (IIP) generated by the superposition of two, *e.g.*, linearly polarized beams (SS, PP) and polarization interference patterns (PIP) by superposition of two linearly polarized beams in orthogonal condition (for instance SP or PS, that is, ±45). In the case of an IIP, there is a variation of light intensity from zero to a maximum value along the grating (optical) period, while in the PIP the intensity of the light is constant over an optical period; the polarization varies locally as shown in **Figure 5a** (distribution of the electrical field vector within the IP relative to topography variation is shown by black arrows).

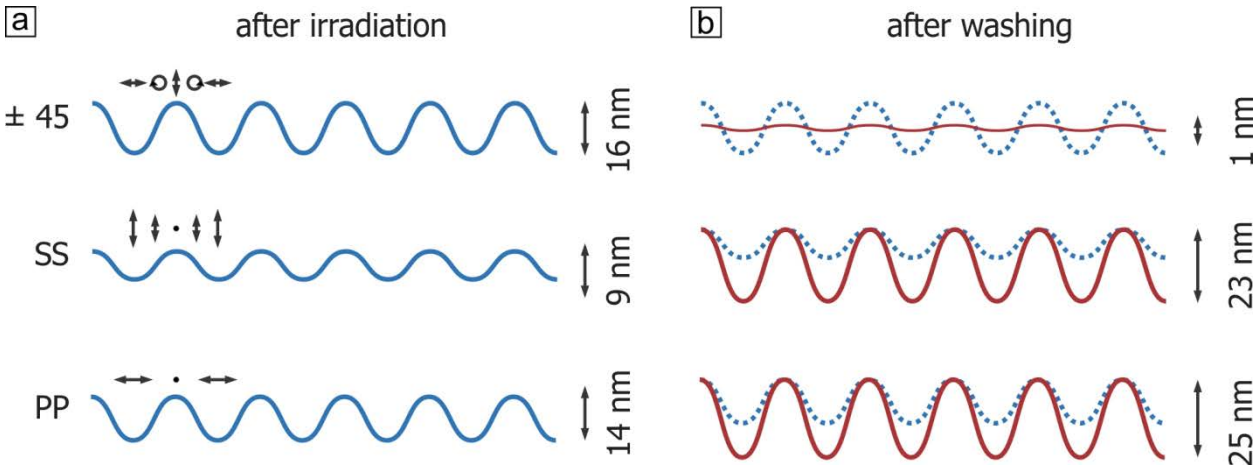


**Figure 5**. (a) AFM cross-sectional profile of the irradiated photosensitive polymer brush (blue lines) for different interference patterns. The "±45" IP represents the polarization combinations IP, and the SS and PP IPs depict the intensity the IP. Local distribution of the electrical field vector relative to the topography is depicted by black arrows. (b) The same cross-sectional profile (red lines) after exposure of the irradiated brush to a good solvent (DMF). The dashed blue lines reproduce the profiles shown in (a) as references.

When comparing the SRG heights just after the irradiation, one may state that the intensity and polarization IPs do not influence significantly the extent of topography altering. Irradiation with PIPs (±45) and IIPs (PP, SS) generates SRGs of several nanometers in height. However, after exposing the just irradiated brush to a good solvent, the changes in grating height depend significantly on the type of the employed IP. In the case of an intensity interference pattern, the SRG increases (red line in **Figure 5b**), while the brush irradiated with the polarization interference pattern features nearly a flat surface after solvent treatment. This can be explained by the fact that under the irradiation with the PIP, the opto-mechanical stresses are generated uniformly across the entire surface, because the intensity of the inscribing light is constant over the optical period. In case of IIP, there are areas of minimum light exposure (see electrical filed distribution depicted in **Figure 5a**), and the brush chains remain bound to the surface due to the lack of opto-mechanical stress.

Until now our intuitively appealing assumption of a partial penetration of surfactant molecules into the brush was superficially supported by characterization of the polymer chain scission during SRG inscription. To scrutinize our assumption of partial penetration of surfactant molecules into the brush more rigorously, we performed a series of nanoFTIR measurements on the polymer brushes before illumination, as well as on the SRGs manufactured via multiple irradiation steps, as described in **Figure 4. Figure 6 c** plots nano-FTIR spectra recorded on the parent PSPMK and on PSPMK brush loaded with azobenzene-containing surfactants. Each spectrum was recorded on a single spot on the SRG surface (blue and red marks in **Figure 6**) and referenced against the spectrum corresponding to the bare Si substrate of the same sample. Each nanoFTIR absorption spectrum was reconstructed from the detected backscattered near field amplitude and phase of the sample; here SRG, and the Si reference, as defined previously. [54, 63] The characteristic vibrational bands from the two compounds can be distinguished: the band of the asymmetric $SO_3$ stretching vibration at 1190 $cm^{-1}$ [64] and the carbonyl stretching vibration at 1730 $cm^{-1}$ [64, 65] are related to PSPMK (**Figures 6a, c**), whereas the symmetric (1346 $cm^{-1}$) and asymmetric (1524 $cm^{-1}$) NO stretches as well as the aromatic C=C mode at 1601 $cm^{-1}$ are due to the surfactant [38, 39, 54] (**Figures 6b, c**). NanoFTIR spectra on the SRGs manufactured by cross illumination in two and three sequential illumination steps (**Figure 4)** are plotted in **Figure 6e and 6g**. It is evident from the comparison of the nanoFTIR spectra representing the two and the three-step illumination that the vibrational bands corresponding to the light-sensitive surfactant at 1346 $cm^{-1}$ ,1524 $cm^{-1}$ and 1601 $cm^{-1}$ are absent after the third illumination step, thus the SRGs are rendered inactive. Furthermore, the spectra recorded at various locations on the SRGs surface, *i.e.*, on the high and low positions (**Figure 6** marked with blue and red respectively),

show no significant variations across the surface – except for the high amplitude pattern – which argues in favor of the identical chemical composition.

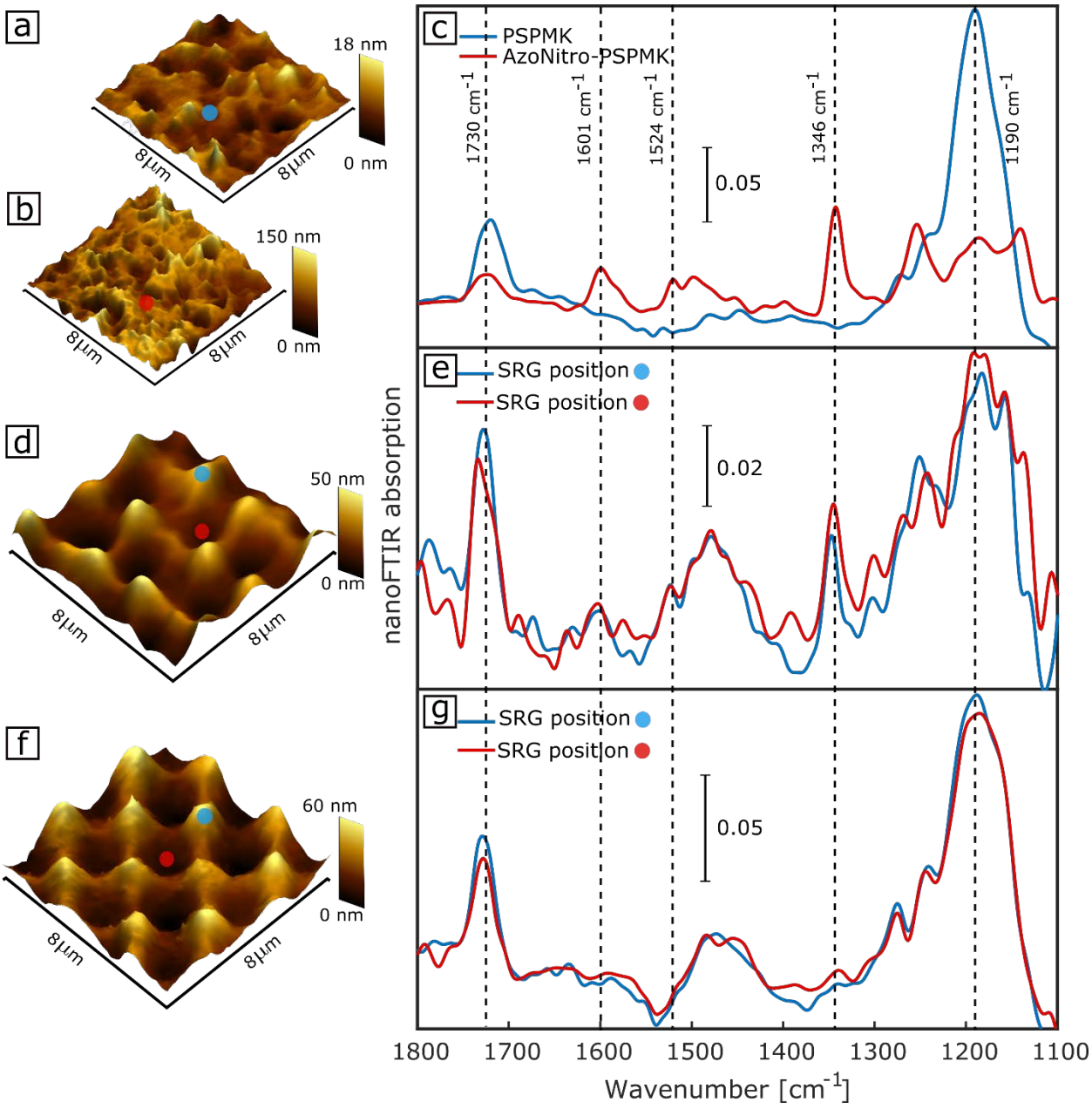


**Figure 6**. AFM topography of an unmodified PSPMK brush (a), a PSPMK brush loaded with light sensitive surfactant (b), SRG after two (d, **Figure 4b**) and three (f, **Figure 4c**) illumination/cleansing steps. (c) Near field spectra of the polymer brush (blue curve) and polymer brush- surfactant complex (red curve). The vibrational bands that correspond to PSPMK are carbonyl stretching vibrations at 1730 $cm^{-1}$ and the asymmetric $SO_3$ stretching vibration at

1190 $cm^{-1}$. The bands arising due to the surfactant are the aromatic C=C mode at 1601 $cm^{-1}$, the asymmetric (1524 $cm^{-1}$) and symmetric (1346 $cm^{-1}$) NO stretch).; (e) and (g) near field spectra of the two different SRG surfaces. In both cases, the spectra were taken at two different positions on the surface (blue and red marks on the topography) corresponding to the location of minimum and maximum height, respectively.

*Reversible switching of the structured brush topography*. The advantage of using polymer brushes in order to shape the topography in the way described above is that the surfactant can, in principle, be removed from the brush at any stage and the nanostructured brush can be used in numerous applications. Here we provide an example where using repeated changes in humidity one can switch the brush topography from structured to flat and back to the initial pattern (**Figure 7a**). During *in-situ* AFM recording the structured photosensitive brush is exposed to water vapor and the polymer grating swells resulting in a flat topography. The subsequent drying procedure restores the original topographical pattern. In case when the topography grating can be inscribed down to the substrate, the topography does not switch back to a flat state but instead generated a topographical pattern with reduced roughness (**Figure 7b**). The fact that the grating develops a depth down to the substrate is possible only if the photosensitive surfactant penetrates the brush completely, which can be achieved by loading weak polyelectrolyte PMAA brushes with photosensitive surfactant by a procedure described elsewhere. [32,45,57]

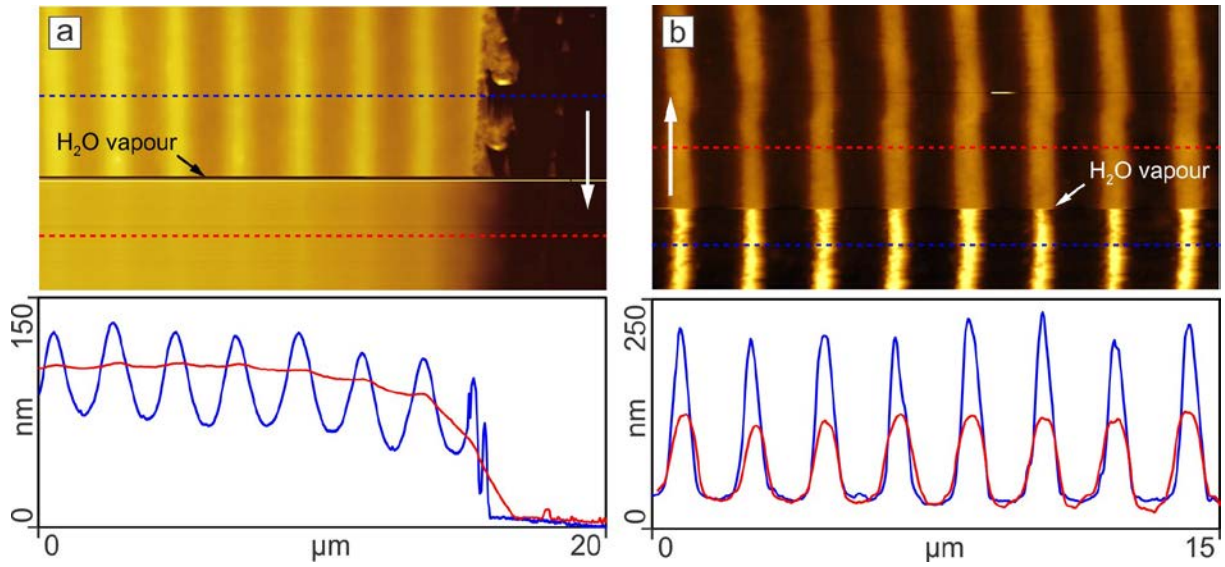


**Figure 7**. AFM micrographs of the swelling experiment of (a) a PSPMK structured brush where the topography grating does not expose the supporting substrate, *i.e.*, from the height minima on there is still a thick layer polymer material left (in this case 155 nm) and (b) PMAA structured brush where grooves expose the bare silicon surface. The blue line represents the grating profile in the dry state, the red line refers to the swollen profile. The scanning direction is from top to bottom as indicated by the white arrow.

## Conclusions

We investigated the complex formation between a strong polyelectrolyte brush made of poly(3-sulfopropyl methacrylate / potassium salt) (PSPMK) and a cationic azobenzene-containing surfactant using AFM and nano-FTIR. . The PSPMK brush was grown from a flat silicon wafer using surface-initiated ATRP reaction. The brush studied used in this study had a grafting density of $\sigma$=0.24 chains/nm$^2$ and a molecular weight of ~570·10$^2$ kDa giving rise to the dry thickness of ~200 nm. Loading the PSPMK brushes with oppositely charged surfactant resulted in film thickness increase to 400 nm. The surfactant rendered the brush photoresponsive and lead to pronounced topography changes under irradiation with various UV interference patterns. Within addition to the well-known phenomenology of forming surface relief gratings, the local scission of the tethered polymer chains was observed after treating the irradiated brush with good

solvent. Here we studied how the extent of polymer chain scission depends on the irradiation dose and the nature of the interference pattern (IP). Moreover, we have found that the cationic surfactant penetrates only the top ~25% of the brush film resulting in the formation of two decoupled layers: a photo-responsive upper layer and a passive, surfactant-free lower layer of ~155 nm thickness. Under irradiation with the IP, the surfactant-free section of the brush remains unaffected by the UV treatment, while the upper photo-responsive layer can be structured many times by successive irradiation cycles employing IPs of different periodicity and direction. Using a home-made near-IR spectroscopic unit combined with an atomic force microscope, we have locally characterized the chemical composition of the polymer brush and confirmed the hypothesis of partial surfactant penetration within the polymer brush film. We have further shown that the photo-structured hydrophilic polymer brush can be reversibly switched between a flat and a structured topography by changing the outside humidity. The advantage of making PE brushes photo-responsive by loading them with azobenzene containing surfactant allows for non-invasive reversible functionalization without the need for complicated (and irreversible) chemical conjugation.

ACKNOWLEDGMENTS: This research is supported by the DFG Priority Program "Microswimmers – From Single Particle Motion to Collective Behaviour" (SPP 1726) and Helmholtz Graduate School on Macromolecular Bioscience (Teltow, Germany). RRP and JG acknowledge financial support from the National Science Foundation under Grant No. DMR-1404639. J.H. acknowledges financial support by the Deutsche Forschungsgemeinschaft (DFG), grant HE 2063/5-1.

**Author information**

ORCID: Rohan R. Patil: 0000-0001-8841-4635

ORCID: Jan Genzer: 0000-0002-1633-238X

## Table of Contents

## Reference


1 Justin O. Zoppe, Nariye Cavusoglu Ataman, Piotr Mocny, Jian Wang, John Moraes, and Harm-Anton Klok, Surface-Initiated Controlled Radical Polymerization: State-of-the-Art, Opportunities, and Challenges in Surface and Interface Engineering with Polymer Brushes, Chemical Reviews 2017 Chem. Rev. 2017, 117, 1105−1318

2 Ayres, N. Polymer brushes: Applications in biomaterials and nanotechnology. Polym. Chem. 2010, 1, 769−777

3 Galvin, C. J.; Genzer, J. Applications of surface-grafted macromolecules derived from post-polymerization modification reactions. Prog. Polym. Sci. 2012, 37, 871−906.

4 Krishnamoorthy, M.; Hakobyan, S.; Ramstedt, M.; Gautrot, J. Surface-Initiated Polymer Brushes in the Biomedical Field: Applications in Membrane Science, Biosensing, Cell Culture, Regenerative Medicine and Antibacterial Coatings. Chem. Rev. 2014, 114, 10976− 11026.

5 Hui, C. M.; Pietrasik, J.; Schmitt, M.; Mahoney, C.; Choi, J.; Bockstaller, M. R.; Matyjaszewski, K. Surface-Initiated Polymerization as an Enabling Tool for Multifunctional (Nano-)Engineered Hybrid Materials. Chem. Mater. 2014, 26, 745−762.

6 Peng, S.; Bhushan, B. Smart polymer brushes and their emerging applications. RSC Adv. 2012, 2, 8557−8578

7 Azzaroni, O. Polymer brushes here, there, and everywhere: Recent advances in their practical applications and emerging opportunities in multiple research fields. J. Polym. Sci., Part A: Polym. Chem. 2012, 50, 3225−3258.

8 M Chen, W. H. Briscoe, S. P. Armes and J. Klein, *Science*, 2009, **323**, 1698

9 J. E. Raynor, J. R. Capadona, D. M. Collard, T. A. Petrie and A. J. Garcia, *Biointerphases*, 2009, **4**, FA3–FA16.

10 J. Pyun, T. Kowalewski and K. Matyjaszewski, *Macromol. Rapid Commun.*, 2003, **24**, 1043

11 W. J. Brittain and S. Minko, *J. Polym. Sci., Part A: Polym. Chem.*, 2007, **45**, 3505.

12 S. T. Milner, *Science*, 1991, **251**, 905.

13 Mittal, V. Polymer brushes substrates, technologies, and properties; Taylor & Francis: Boca Raton, FL, 2012; p 340.

14 *Polymer Brushes: Synthesis, Characterization, Applications*; Advincula, R. C., Brittain, W. J., Caster, K. C., Rühe, J., Eds.; Wiley-VCH Verlag GmbH & Co. KGaA: Weinheim, 2004.

15 Pincus, P. Macromolecules 1991, 24, 2912

16 Ballauff, M.; Borisov, O. Polyelectrolyte Brushes. Curr. Opin. Colloid Interface Sci. 2006, 11 (6), 316.

17 Gong, P.; Genzer, J.; Szleifer, I. Phys. Rev. Lett. 2007, 98, 018302

18 Kumar, R.; Sumpter, B. G.; Kilbey, S. M. J. Chem. Phys. 2012, 136, 234901.

19 Gong, P.; Wu, T.; Genzer, J.; Szleifer, I. Macromolecules 2007, 40, 8765.

20 W.-L. Chen, R. Cordero, H. Tran, C. K. Ober, Macromolecules 2017, 50, 4089–4113

21 Christau, S.; Thurandt, S.; Yenice, Z.; von Klitzing, R. Stimuli-Responsive Polyelectrolyte Brushes as a Matrix for the Attachment of Gold Nanoparticles: The Effect of Brush Thickness on Particle Distribution. *Polymers* **2014**, *6*, 1877–1896.

22 Kesal, D.; Christau, S.; Krause, P.; Möller, T.; von Klitzing, R. Uptake of pH-Sensitive Gold Nanoparticles in Strong Polyelectrolyte Brushes. *Polymers* **2016**, *8*, 134

23 Pyshkina O, Sergeyev V, Zezin A, Kabanov V, Gage D, Stuart MC. The Effect of Grafting Density on Binding Isotherms of Cationic Surfactants to a Polyacrylic Acid Brush. Langmuir 2003;19:2000–6. doi:10.1021/la020457h.

24 Konradi R, Rühe J. Binding of Oppositely Charged Surfactants to Poly(methacrylic acid) Brushes. Macromolecules 2005;38:6140–51. doi:10.1021/ma047692m.

25 Döbbelin M, Arias G, Loinaz I, Llarena I, Mecerreyes D, Moya S. Tuning Surface Wettability of Poly(3-sulfopropyl methacrylate) Brushes by Cationic Surfactant-Driven Interactions. Macromol Rapid Commun 2008;29:871–5. doi:10.1002/marc.200800071.

26 Rosenfeldt S, Wittemann a., Ballauff M, Breininger E, Bolze J, Dingenouts N. Interaction of proteins with spherical polyelectrolyte brushes in solution as studied by small-angle x-ray scattering. Phys Rev E 2004;70:061403. doi:10.1103/PhysRevE.70.061403.

27 Leermakers FAM, Ballauff M, Borisov O V. On the mechanism of uptake of globular proteins by polyelectrolyte brushes: a two-gradient self-consistent field analysis. Langmuir 2007;23:3937–46. doi:10.1021/la0632777.

28 Dai J, Bao Z, Sun L, Hong SU, Baker GL, Bruening ML. High-capacity binding of proteins by poly(acrylic acid) brushes and their derivatives. Langmuir 2006;22:4274–81. doi:10.1021/la0600550.

29 Mei Y, Lu Y, Polzer F, Ballauff M, Drechsler M. Catalytic Activity of Palladium Nanoparticles Encapsulated in Spherical Polyelectrolyte Brushes and Core−Shell Microgels. Chem Mater 2007;19:1062–9. doi:10.1021/cm062554s.

30 Schrinner M, Proch S, Mei Y, Kempe R, Miyajima N, Ballauff M. Stable Bimetallic Gold–Platinum Nanoparticles Immobilized on Spherical Polyelectrolyte Brushes: Synthesis, Characterization, and Application for the Oxidation of Alcohols. Adv Mater 2008;20:1928–33. doi:10.1002/adma.200702421.

31 Schuh C, Rühe J. Penetration of Polymer Brushes by Chemical Nonidentical Free Polymers. Macromolecules 2011;44:3502–10. doi:10.1021/ma102410z.

32 Kopyshev A, Galvin CJ, Genzer J, Lomadze N, Santer S. Opto-mechanical scission of polymer chains in photosensitive diblock-copolymer brushes. Langmuir 2013;29:13967–74. doi:10.1021/la403241t.

33 Zakrevskyy Y, Roxlau J, Brezesinski G, Lomadze N, Santer S. Photosensitive surfactants: Micellization and interaction with DNA. J Chem Phys 2014;140:044906. doi:10.1063/1.4862678.

34 Santer, S. «Remote control of soft nano-objects by light using azobenzene containing surfactants» Journal of Physics D: Applied Physics, 51 (2017) 013002.

35 Rau H. Photoisomerization of azobenzenes. In: Rabek J, editor. Photochem. Photophysics, Boca Raton, FL: CRC Press; 1990, p. 119–42.

36 Rochon P, Batalla E, Natansohn A. Optically induced surface gratings on azoaromatic polymer films. Appl Phys Lett 1995;66:136–8. doi:10.1063/1.113541.

37 Kim DY, Li L, Jiang XL, Shivshankar V, Kumar J, Tripathy SK. Polarized Laser Induced Holographic Surface Relief Gratings on Polymer Films. Macromolecules 1995;28:8835–9. doi:10.1021/ma00130a017.

38 Lomadze N, Kopyshev A, Rühe J, Santer S. Light-Induced Chain Scission in Photosensitive Polymer Brushes. Macromolecules 2011; 44:7372–7. doi:10.1021/ma201016q.

39 Schuh C, Lomadze N, Rühe J, Kopyshev A, Santer S. Photomechanical degrafting of azo-functionalized poly(methacrylic acid) (PMAA) brushes. J Phys Chem B 2011;115:10431–8. doi:10.1021/jp2041229.

40 V. Toshchevikov, J. Ilnytskyi, M. Saphiannikova, *J. Phys. Chem. Lett.* **2017**, *8*, 1094.

41 N.S. Yadavalli, D. Korolkov, J. Moulin, M. Krutyeva, S. Santer, *ACS Appl. Mater. Interfaces* **2014**, *6*, 11333.

42 N.S. Yadavalli, F. Linde, A. Kopyshev, S. Santer, *ACS Appl. Mater. Interfaces* **2013**, *5*, 7743.

43 G. Di Florio, E. Bründermann, N.S. Yadavalli, S. Santer and M. Havenith, *Nano Lett.* **2014**, *14*, 5754.

44 J. Ilnytskyi, M. Saphiannikova, *Chem. Phys. Chem.* **2015**, *16*, 3180.

45 Kopyshev, A.; Lomadze, N.; Feldmann, D., Genzer, J.; Santer, S. «Making Polymer Brush Photosensitive with Azobenzene Containing Surfactants» Polymer, 79 (2015) 65–72

46 See for instance review: Xin Xu, Mark Billing, Marina Ruths, Harm-Anton Klok, and Jing Yu, Structure and Functionality of Polyelectrolyte Brushes: A Surface Force Perspective, Chem. Asian J. 2018, 13, 3411 – 3436

47 Israëls, R.; Leermakers, F.A. M.; Fleer, G. J. Macromolecules

1994, 27, 3087.

48 Lyatskaya, Yu. V.; Leermakers, F.A. M.; Fleer, G. J.; Zhulina, E. B.; Birshtein, T. M. Macromolecules 1995, 28, 3562.

49 Zhulina, E. B.; Birshtein, T. M.; Borisov, O. V. Macromolecules 1995, 28, 1491

50O. V. Borisov, T. M. Birshtein, E. B. Zhulina, J. Phys. II 1991, 1, 521–526;

51 O. V. Borisov, E. B. Zhulina, T. M. Birshtein, Macromolecules 1994, 27, 4795–4803

52 Xiao Xu, Stefano Angioletti-Uberti, Yan Lu, Joachim Dzubiella, and Matthias Ballauff, Interaction of Proteins with Polyelectrolytes: Comparison of Theory to Experiment DOI: 10.1021/acs.langmuir.8b01802

53 Brehm, M., Taubner, T., Hillenbrand, R. & Keilmann, F. Infrared spectroscopic mapping of single nanoparticles and viruses at nanoscale resolution. *Nano Lett.* **6,** 1307–1310 (2006).

54 Huth, F. *et al.* Nano-FTIR absorption spectroscopy of molecular fingerprints at 20 nm spatial resolution. *Nano Lett.* **12,** 3973–3978 (2012).

55 Amarie, S., Ganz, T. & Keilmann, F. Mid-infrared near-field spectroscopy. *Opt. Express* **17,** 21794–21801 (2009).

56 Ocelic, N., Huber, A. & Hillenbrand, R. Pseudoheterodyne detection for background-free near-field spectroscopy. *Appl. Phys. Lett.* **89,** 2004–2007 (2006).

57 Govyadinov, A. a., Amenabar, I., Huth, F., Carney, P. S. & Hillenbrand, R. Quantitative Measurement of Local Infrared Absorption and Dielectric Function with Tip-Enhanced Near-Field Microscopy. *J. Phys. Chem. Lett.* **4,** 1526–1531 (2013).

58 Konradi, R. and Rühe, J. Binding of Oppositely Charged Surfactants to Poly(methacrylic acid) Brushes *Macromolecules* **2005**, *38*, 6140–6151.

59 Kopyshev, A.; Galvin, C.J.; Patil, R.R.; Genzer, J.; Lomadze, N.; Feldmann, D.; Zakrevski, J.; Santer, S. «Light-induced reversible change of roughness and thickness of photosensitive polymer brushes» ACS Applied Materials & Interfaces, 8 (2016) 19175–19184

60 O.V. Borisov, T.M. Birstein, E.B. Zhulina, J. Phys. II **1**, 521 (1991)

61 Matthias Ballauff, Oleg Borisov Polyelectrolyte brushes, Current Opinion in Colloid & Interface Science Volume 11, Issue 6, December 2006, Pages 316-323

62 Kopyshev, A.; Galvin, C. J.; Genzer, J.; Lomadze, N.; Santer, S. «Polymer brushes modified by photosensitive azobenzene containing polyamines» Polymer, 98 (2016) 421-428.

62 Amenabar, I. *et al.* Structural analysis and mapping of individual protein complexes by infrared nanospectroscopy. *Nat. Commun.* **4,** 2890 (2013).

63 Kästner, B. *et al.* Infrared Nanospectroscopy of Phospholipid and Surfactin Monolayer Domains. *ACS Omega, 10.1021/acsomega.7b01931* (2018). doi:10.1021/acsomega.7b01931

64 Muller, E. A., Pollard, B. & Raschke, M. B. Infrared Chemical Nano-Imaging : Accessing Structure , Coupling , and Dynamics on Molecular Length Scales. (2015). doi:10.1021/acs.jpclett.5b00108

65 Berweger, S. *et al.* Nano-chemical infrared imaging of membrane proteins in lipid bilayers. *J. Am. Chem. Soc.* **135,** 18292–18295 (2013).

66 Yoxall, E., Schnell, M., Mastel, S. & Hillenbrand, R. Magnitude and phase-resolved infrared vibrational nanospectroscopy with a swept quantum cascade laser. *Opt. Express* **23,** 13358 (2015).

70. Brehm, M., Taubner, T., Hillenbrand, R. & Keilmann, F. Infrared spectroscopic mapping of single nanoparticles and viruses at nanoscale resolution. *Nano Lett.* **6,** 1307–1310 (2006).

71. Pfitzner, E. *et al.* Near-field magneto-caloritronic nanoscopy on ferromagnetic nanostructures. **125329,** (2018).

[63] Mastel, S. *et al.* Nanoscale-resolved chemical identification of thin organic films using infrared near- field spectroscopy and standard Fourier transform infrared references Nanoscale-resolved chemical identification of thin organic films using infrared near-field spectros. *Appl. Phys. Lett.* **106,** 23113 (2015).

[64] Ramstedt, M. *et al.* Synthesis and Characterization of Poly ( 3-Sulfopropylmethacrylate ) Brushes for Potential Antibacterial Applications Synthesis and Characterization of Poly ( 3-Sulfopropylmethacrylate ) Brushes for Potential Antibacterial Applications. *Synthesis (Stuttg).* 10192–10199 (2007). doi:10.1021/la062670

[65] Taubner, T., Hillenbrand, R. & Keilmann, F. Nanoscale polymer recognition by spectral signature in scattering infrared near-field microscopy. *Appl. Phys. Lett.* **85,** 5064 (2004).